Ectopic sonic hedgehog signaling impairs telencephalic dorsal midline development: implication for human holoprosencephaly

Xi Huang, Ying Litingtung and Chin Chiang∗

Department of Cell and Developmental Biology, Vanderbilt University Medical Center,
4114 MRB III, Nashville, TN 37232, USA

Holoprosencephaly (HPE) is the most common developmental anomaly of the human forebrain, and in its severe form, the cerebral hemispheres fail to completely separate into two distinct halves. Although disruption of ventral forebrain induction is thought to underlie most HPE cases, a subset of HPE patients exhibits preferential dysgenesis of forebrain dorsal midline structures with unknown etiology. In this study, we show that Sonic hedgehog (Shh) lacking cholesterol moiety in one allele (*ShhN/+*) in mice can elicit ectopic Shh signaling in early telencephalon to induce ventral progenitor marker expression in the cortical region and impair telencephalic dorsal midline development. Prolonged ectopic ShhN signaling impaired Bmp and Wnt signaling from the dorsal patterning center through upregulation of *Fgf8*, leading to augmented cell proliferation, decreased cell death and impaired roof plate morphogenesis. Accordingly, *ShhN/+* mutant telencephalic dorsal midline structures, including cortical hem, hippocampus and choroid plexus, either failed to form or were hypoplastic. Strikingly, *ShhN/+* mutants displayed a spectrum of phenotypic features such as failure of anterior cerebral hemisphere to divide, hydrocephalus and cleft palate which have been observed in a human patient with milder HPE predicted to produce SHHN protein due to a truncation mutation in one *SHH* allele. We propose that elevated ectopic Shh signaling can impair dorsal telencephalic midline morphogenesis, and lead to non-cleavage of midline structures mimicking human HPE with dorsal midline defects.

INTRODUCTION

The telencephalon, the most anterior portion of the developing neural tube, can be generalized into two subdivisions, the pallium and subpallium. Secreted molecules generated by patterning centers extending from the embryonic telencephalic midline induce and maintain the molecular identities of each subdivision (1–3). Within the subpallium, development of the medial ganglionic eminence (MGE) and lateral ganglionic eminence (LGE), which largely make up the anlage of the basal ganglia, requires Shh secreted initially from the prechordal plate and subsequently from the ventral telencephalic midline (4–6). Loss of Shh signaling in these ventral patterning centers leads to impaired ganglionic eminence development at the expense of dorsal cell types (6), whereas ectopic Shh signaling in the cortex can induce ventral telencephalic marker gene expressions (7,8).

The roof plate is a dorsal patterning center that organizes the development of the dorsal and medium pallium, including the hippocampus and choroid plexus (9). The BMP subfamily of the TGFβ superfamily plays a critical role in patterning the dorsal neural tube (10). Multiple *Bmp* genes are expressed in the roof plate of the telencephalon (11) and mice deficient in type I Bmp receptor BmprIa or with ablation of Gdf7 (Bmp12)-expressing cells display abnormal choroid plexus development (12,13), consistent with a primary role of Bmps in dorsal telencephalic patterning. The Wnt-rich cortical hem lying dorsal to the choroid plexus and ventral to the hippocampus has been proposed to provide patterning cues to both the developing hippocampus and choroid plexus (14). Targeted inactivation of *Wnt3a*, or the downstream Wnt signaling co-factor *Lef-1*, severely impairs hippocampal development (15,16), whereas early inactivation of β-catenin, a key mediator of

---

*To whom correspondence should be addressed. Tel: +1 6153434922; Fax: +1 6159363475; Email: chin.chiang@vanderbilt.edu

canonical Wnt signaling in the telencephalon, leads to disrupted growth of the hippocampus and choroid plexus (17). The current model suggests that Fgf8 expressed in the anterior margin of the telencephalon functions to coordinate the cross-regulation between dorsal and ventral patterning centers. Specifically, ventrally derived Shh promotes and maintains the proper dose of Fgf8 signaling, which in turn maintains a balance of dorsally derived Bmp and Wnt signaling to modulate telencephalic outgrowth and patterning (2,18).

Holoprosencephaly (HPE) is the most common developmental anomaly of the human forebrain, and in its severe form, the cerebral hemispheres fail to separate into two distinct halves (19–21). It is thought that disturbance of ventral forebrain induction underlies the disruption of hemispheric bifurcation. Consistent with this model, human patient studies have identified a battery of mutations involved in the SHH and NODAL signaling pathways, both of which are required for proper ventral forebrain patterning (21,22). However, these studies do not explain the observation that some HPE patients suffer from failure of hemispheric division, yet have relatively normal ventral brain structures, notably those with a condition known as Middle Interhemispheric Holoprosencephaly (MIH), a recognizable variant of HPE with differing clinical prognosis (23–26). Since mutation in human ZIC2, a zinc finger protein homologous to *Drosophila* odd-paired, has been identified in one MIH patient and knockdown of mouse *Zic2* expression leads to deregulation of roof plate cell proliferation and apoptosis (27,28), ZIC2 mutations have been generally associated with the MIH syndrome (23). However, predominantly, ZIC2 mutations are associated with classical HPE (27), and given the heterogeneity of MIH and the lack of *Zic2* mutations in many MIH patients, it is unlikely that ZIC2 mutations underlie the etiology of MIH in many patients.

We have previously generated mice expressing non-cholesterol-modified Shh (ShhN) and demonstrated that ShhN can spread far from its site of synthesis to elicit ectopic Shh pathway activation in the limb bud (29). In this study, we show that persistent ectopic ShhN signaling in the dorsal telencephalon severely alters Bmp and Wnt signaling from dorsal patterning centers that are crucial for proper dorsal midline development, resulting in altered behavior of roof plate cells and impaired roof plate invagination. Hence, the cortical hem does not form and

development of the choroid plexus and hippocampus is severely disrupted. Strikingly, we found that *ShhN*/+ mice exhibited a spectrum of phenotypic features such as partial division of cerebral hemispheres, hydrocephalus and cleft palate (CLP) while their external craniofacial features were largely unaffected. All of these characteristics were observed in a human patient with milder HPE and predicted to produce SHHN protein due to a truncation mutation in one SHH allele. Thus, our results suggest a novel mechanism by which ectopic Shh signaling impairs dorsal forebrain development, resulting in non-cleavage of midline structures. In addition, our study may shed light on the molecular pathogenesis of MIH, a variant of HPE that preferentially shows disruption of telencephalic dorsal midline structures.

RESULTS

ShhN/+ telencephalon displays early morphological defects

Starting from E10.5, *ShhN*/+ embryos exhibited several distinct morphological differences when compared with wild-type, such as enlarged brain ventricles and widely separated telencephalic ventricles (Fig. 1A, A′, C, C′). H&E-stained coronal sections of E10.5 telencephalon revealed that *ShhN*/+ dorsal midline failed to invaginate, which is apparent in wild-type. In contrast, development of the ventral MGE, was morphologically comparable at this stage between wild-type and *ShhN*/+ (Fig. 1B, B′). At E12.5, *ShhN*/+ telencephalon lacked the characteristic thickened hippocampal neuroepithelium found in the dorsal midline (Fig. 1D, D′). In addition to MGE and LGE at their respective locations, the appearance of a third eminence with LGE character was evident in the mutant (labeled as double-asterisks in Fig. 1D′, see below).

ShhN/+ telencephalic roof plate displays increased proliferation and reduced apoptosis

The invagination and remodeling of the telencephalic dorsal midline is normally accompanied by reduced roof plate cell proliferation and increased cell death (11,28). To determine whether these cellular properties are associated with the failure of dorsal midline down-growth in *ShhN*/+, we performed cell proliferation and apoptosis analysis of the dorsal

Figure 1. *ShhN*/+ telencephalon displays early dorsal midline defects (A, A′). Dorsal–frontal views of E10.5 wild-type (**A**) and *ShhN*/+ (**A′**) embryos. Note the widely separated telencephalic ventricles by expanded dorsal midline tissue in *ShhN*/+. (**B, B′**) Coronal sections of E10.5 telencephalons show defective down-growth of *ShhN*/+ dorsal midline (arrowhead in B) compared with wild-type (arrowhead in B′). (**C, C′**) Lateral views of E12.5 embryos reveal enlarged brain ventricles in *ShhN*/+ mutants (C′), indicative of hydrocephalus. (**D, D′**) Coronal sections of E12.5 wild-type (D) and *ShhN*/+ (D′) telencephalon. In addition to persistent defects in dorsal midline invagination, the presence of a third eminence (labeled as double-asterisks) positioned between the second ventral eminence (labeled as asterisks) and cortical region is also evident in *ShhN*/+ telencephalon (asterisk in D′). (**E, E′, G, G′, I, I′, H**) Roof plate cell proliferation analysis. Proliferation index shown in (**M**) is the percentage of BrdU-positive cell numbers over total cell numbers highlighted by DAPI staining. Dorsal midline cell proliferation index was comparable between wild-type (E) and *ShhN*/+ (E′) at E9.5. Compared with surrounding cortical region, cell proliferation is reduced in the roof region of E10.0 wild-type (G, data not shown). *ShhN*/+ roof plate cells show about 1.8-fold higher proliferation index when compared with wild-type control (G′, M). Similarly, enhanced roof plate cell proliferation was found in *ShhN*/+ at E10.5 (I, I′, M). White bracket denotes a central region of the roof plate. (**F, F′, H, H′, J, J′, N**) Roof plate cell death analysis. Cell death index shown in (N) is the percentage of TUNEL-positive cell numbers over total cell numbers highlighted by DAPI staining. Roof plate cells normally display high apoptotic activity, whereas very little apoptosis is observed in other telencephalic regions (F, H, J and data not shown). However, most *ShhN*/+ roof plate cells fail to undergo apoptosis and show significantly reduced cell death index when compared with wild-type at E9.5, E10.0 and E10.5 (F′, H′, J′, N). (**K, K′, L, L′**) Yellow spots observed in (H, J, J′) were auto-fluorescent blood cells. Expression of Lhx5 protein, a roof plate progenitor cell marker, is significantly expanded in E10.0 *ShhN*/+ dorsal midline (K′, **O**) when compared with wild-type (K, O). Similarly *Lhx5* mRNA expression domain is also significantly expanded in the mutant at E13.5 (compare L and L′).
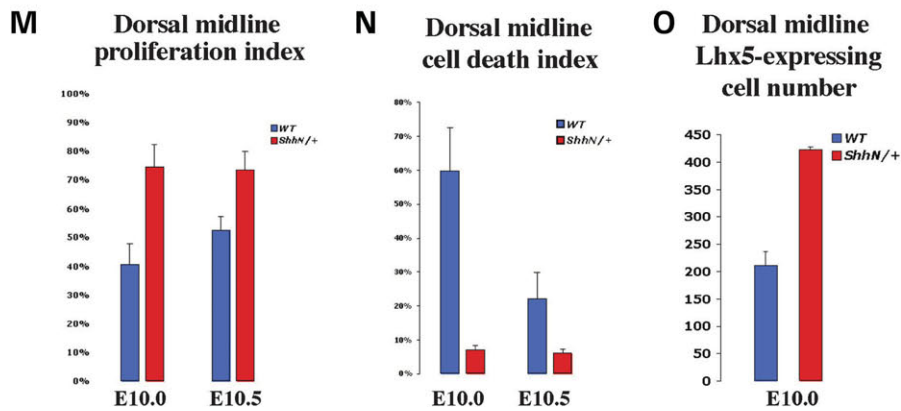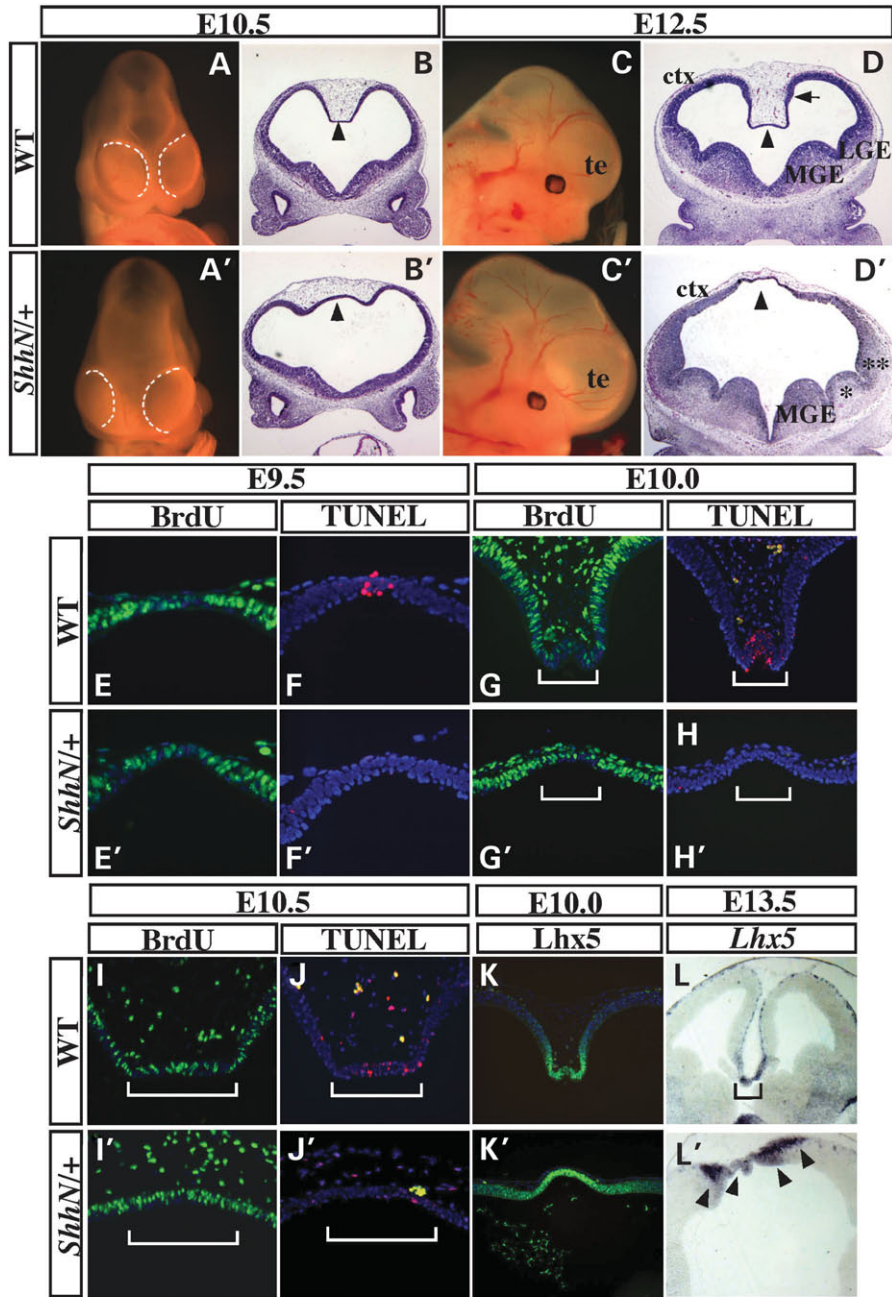
midline neuroepithelium. At E9.5, a stage prior to dorsal midline invagination, we detected prominent apoptotic activity at the most dorsal-medial tissue in wild-type telencephalon. In contrast, apoptosis was essentially eliminated in *ShhN*/+ dorsal midline (Fig. 1F, F′), although cell proliferation was not significantly different from wild-type in this region (Fig. 1E, E′). At E10, differential proliferation was observed in wild-type dorsal telencephalon with reduced proliferation in the roof plate region compared with adjacent neuroepithelium. However, in *ShhN*/+, cell proliferation in the roof region was comparable to adjacent tissues and significantly higher when compared with wild-type (*ShhN*/+ roof cell proliferation index was approximately 1.8-fold higher) (Fig. 1G, G′, M). Similarly, significantly reduced apoptosis was detected in the *ShhN*/+ roof region (more than 7-fold lower) compared with wild-type (Fig. 1H, H′, N). The augmented proliferation and reduced apoptosis in the mutant dorsal midline persisted at E10.5 (Fig. 1I, I′, J, J′, M, N). *Lhx5*, a member of the LIM homeobox gene family encoding a transcription factor, is normally expressed in the roof plate progenitors, but not in the choroid plexus or cortical hem (30,31). We found that the Lhx5-expressing domain expanded in *ShhN*/+ dorsal telencephalic region as early as E10 with more than 2-fold increase in cell number, which persisted to E13.5, indicating a significant expansion of roof plate progenitor cell population (Fig. 1K, K′, L, L′, O; Supplementary Material, Fig. S1). We conclude that defective dorsal midline development in *ShhN*/+ is attributed to increased cell proliferation and reduced cell death in the roof plate region, resulting in expansion of the roof plate progenitor pool. These defects may also lead to failure of tissue invagination.

ShhN/+ telencephalon shows expansion of the basal ganglionic eminences

To examine dorsoventral patterning in *ShhN*/+ telencephalon, we performed molecular marker analyses at stages when the telencephalon displays distinct regional patterns. *Pax6*, a homeobox gene that represses *Nkx* expression and is itself repressed by Shh signaling (32), is uniformly expressed in the cortical region of the telencephalon. However, at E12.5, Pax6 expression showed non-uniform and a more dispersed pattern in *ShhN*/+ embryos (Fig. 2A, A′). By E13.5, the reduction in Pax6 expression domain became most evident (Fig. 2H, H′). Additional dorsal pallium markers, *Ngn2* and *Emx2*, showed similarly reduced expression domain and intensity, indicative of severe dorsal patterning defects. In contrast to the loss of cortical progenitors, we observed dorsal expansion of markers indicative of ventral telencephalic progenitors in *ShhN*/+. The expression of Nkx2.1 is normally restricted to the MGE domains (Fig. 2B), but in *ShhN*/+ Nkx2.1-positive cells expanded to the ventral portion of the second ganglionic eminence where LGE normally forms (arrowheads in Fig. 2B′). This observation is consistent with the expanded *Shh* expression domain up to the second eminence (see below). *Mash1*, which encodes a pro-neural basic helix-loop-helix transcription factor, is expressed in the pan-ventral telencephalic region, including both MGE and LGE (33–35). Previous studies have shown that exogenous Shh is capable of eliciting ectopic LGE markers including Mash1 expression in naïve telencephalic

explants (8,36). We found that Mash1 expression expanded dorsally encompassing the ectopic third eminence and scattered sites within the cortical region of *ShhN*/+ telencephalon (Fig. 2C, C′, D, E, E1, E2). Notably, a significant portion of ectopic Mash1-expressing cells also expressed Gsh2 (Fig. 2F1, F2), an Shh-dependent inducible transcription factor normally expressed in the MGE and LGE (37). This is in contrast to wild-type where co-expressing cells were restricted to the basal ganglionic eminences (Fig. 2F). Since Isl1 is expressed in differentiating neurons within the subventricular zone and mantle zone of the LGE (38), we further performed Isl1 immunostaining (Fig. 2G, G1, G2), showing that *ShhN*/+ cortical region also contained differentiated neurons of LGE identity. Taken together, we conclude that the LGE and, to a lesser extent, MGE are expanded at the expense of the cortical domain in *ShhN*/+ telencephalon.

The development of hippocampus, choroid plexus and cortical hem is defective in *ShhN*/+ telencephalon

The observation that *ShhN*/+ telencephalon failed to invaginate and lacked morphologically distinguishable dorsal midline suggests that the generation of midline-derived structures is affected. To determine the extent of dorsal midline morphogenesis defects, regional marker analyses were performed at E13.5 when dorsal midline structures and their molecular identities are well established. Previous studies demonstrated that *Bmp4* and *Bmp7* expressions normally mark the choroid plexus (11,39). We found that expression of these two *Bmp* genes in *ShhN*/+ dorsal telencephalic epithelium was barely detectable, while persistent *Bmp7* expression was found in the dorsal medial mesenchyme (Fig. 3A, A′, B, B′). Also, *ShhN*/+ exhibited no expression of definitive choroid plexus marker *transthyretin* (*Ttr*) (Fig. 3C, C′), suggesting a failure of choroid plexus specification at this stage. While the expression of *Wnt2b* normally marks the Wnt-rich cortical hem (15,39), its transcript was not detectable in *ShhN*/+ mutants (Fig. 3D, D′). *Wnt5a* expression, which encompasses the cortical hem and mesenchyme underneath the hippocampus and distal cortex, was also severely affected in *ShhN*/+ mutants (Fig. 3E, E′). Similarly, expression of the Wnt pathway component *Lef1* diminished considerably in *ShhN*/+ mutants, in contrast to its normal expression in the choroid plexus and hippocampus (Fig. 3F, F′). Taken together, we conclude that the development of the hippocampal primordium, cortical hem and choroid plexus is significantly compromised in *ShhN*/+ mutants.

ShhN elicits ectopic signaling throughout *ShhN*/+ telencephalic neuroepithelium

In order to assess Shh signaling in wild-type and *ShhN*/+ telencephalon, we utilized *Patched-LacZ* mice, in which β-galactosidase activity indicates Shh signaling activity (40). At E10.5, coronal sections through the MGE region revealed that while Shh signaling activity was confined within the MGE of wild-type telencephalon, ShhN could evoke signaling activity dorsal to the morphological boundary of MGE in *ShhN*/+ mutants (Fig. 4D, D′). However, we could not
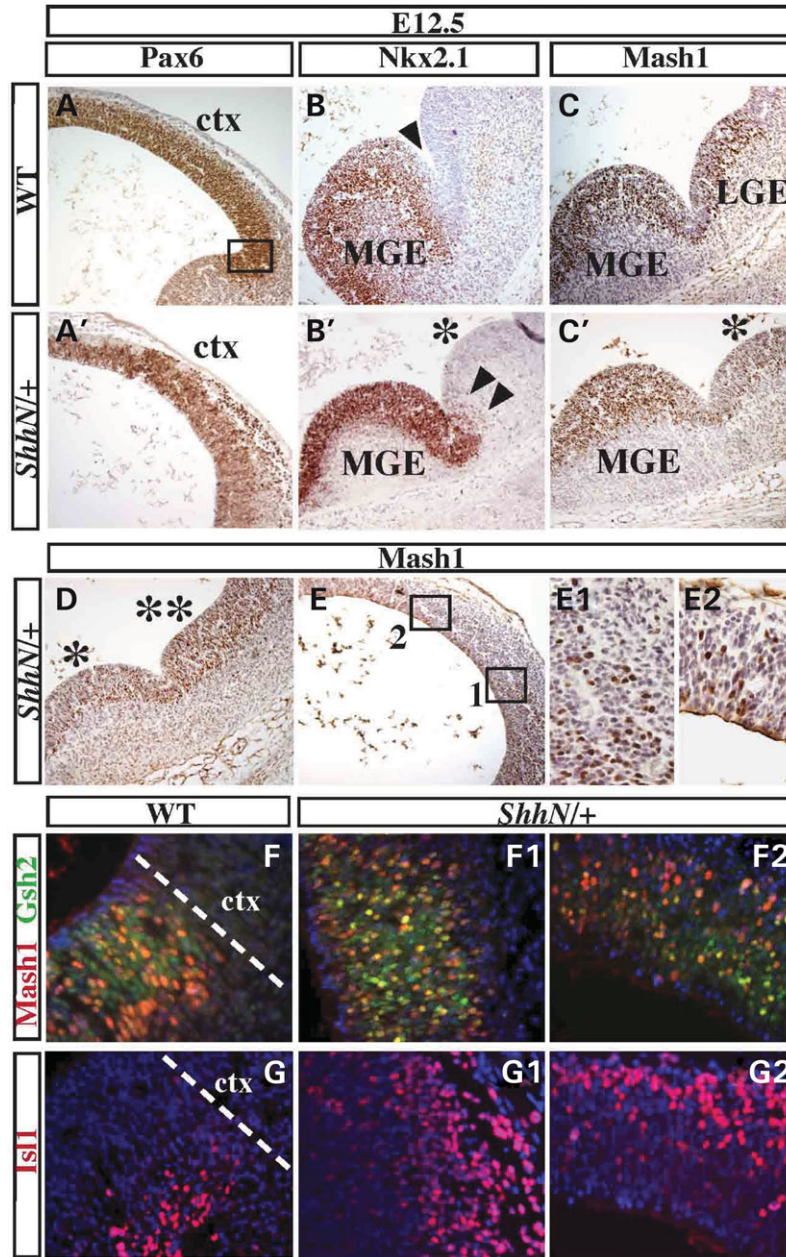
Figure 2. MGE and LGE domains are expanded in *ShhN*/+ telencephalon (A, A′). Pax6 expression pattern of E12.5 wild-type and *ShhN*/+ cortical region. Pax6+ cells are scattered throughout the *ShhN*/+ cortex (**A′**), while uniform Pax6 expression demarcates the cortical region in wild-type (**A**). (**B**, **B′**) Nkx2.1 expression pattern of E12.5 wild-type and *ShhN*/+ MGE region. Nkx2.1, an MGE-specific marker that defines the most ventral-medial eminence in wild-type (B) extends into the ventral portion of the second eminence (asterisk) of *ShhN*/+ (B′). (**C**, **C′**, **D**, **E**, E1, E2) Mash1 expression in wild-type (C) and *ShhN*/+ (C′, D, E, E1, E2). Mash1, an LGE marker, is detected in the ectopic third eminence (double asterisk in D) and at scattered sites along the cortical region (E, E1, E2), indicative of an expanded LGE territory in *ShhN*/+. (E1) and (E2) are magnified views of boxed areas 1 and 2 in (E), respectively. A significant portion of Gsh2 and Mash1 were co-expressed at ectopic sites in the cortical region of *ShhN*/+ telencephalon (F1, F2), in contrast to wild-type where co-expressing cells were restricted to the basal ganglionic eminences (**F**). Differentiated ventral LGE marker Isl1 is also ectopically expressed at the *ShhN*/+ cortical region, in contrast to its restricted expression in the differentiating neurons within the subventricular zone and mantle zone in wild-type (**G**, G1, G2), indicating that *ShhN*/+ cortical region also contains differentiated neurons of ventral LGE identity. The locations of F1/G1 and F2/G2 approximately correspond to boxed areas 1 and 2 in (E), respectively. (**H**, **H′**, **I**, **I′**, **J**, **J′**, **K**, **K′**) Expression of *Pax6*, *Ngn2* and *Emx2* in wild-type and *ShhN*/+ telencephalon.

detect expanded ShhN protein by immunohistochemistry possibly due to a level that is below detection threshold (Fig. 4B, B′). By E13.5, ectopic ShhN signaling activity was detected throughout the *ShhN*/+ telencephalic neuroepithelium in contrast with Shh signaling being restricted to the ventral telencephalon in wild-type (Fig. 4E, E′). In addition, we found that the domain of *Shh* transcript in the ventral telencephalic region and zona limitans intrathalamica (zli) at E10.5 appears to be slightly expanded in *ShhN*/+ (Fig. 4A, A′). This expansion becomes more evident at E13.5 when
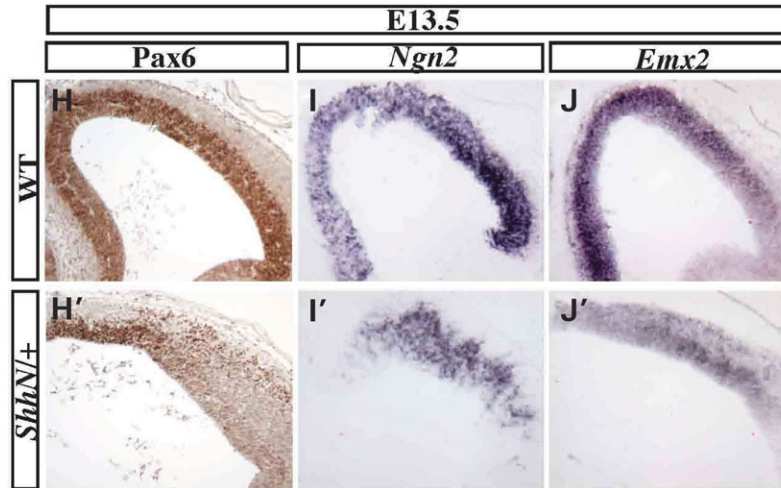
Figure 2. Continued.

we found a small number of Shh-expressing cells extending beyond the morphological boundary of the MGE into the ventral portion of the adjacent eminence (Fig. 4C, C′), consistent with expanded Nkx2.1 expression (Fig. 2B′). Another indicator of Shh pathway activation is the accumulation of the zinc finger transcription factor, Gli3, by inhibiting the formation of its repressor forms (41,42). Therefore, we determined the relative amount of Gli3 repressor (Gli3R) to Gli3 full length (Gli3−190) as another readout of Shh signaling. Consistent with widespread *Ptch1* reporter expression, we observed more than 30% reduction in Gli3/Gli3−190 ratio in E13.5 whole brain extracts of *ShhN/+* mutants when compared with wild-type (Fig. 4F). Taken together, with the ectopic MGE and LGE marker expressions, we conclude that the *ShhN/+* telencephalic neuroepithelium is subject to globally expanded ShhN signaling along the dorsal–ventral axis.

Ectopic ShhN signaling impairs dorsal telencephalic Bmp and Wnt signaling through upregulation of *fgf8*

In order to gain insight into the mechanism by which ectopically enhanced ShhN signaling affects dorsal telencephalic patterning, we examined the expression of multiple essential components of the Fgf, Bmp and Wnt signaling pathways that work in concert to regulate regional identities and growth (2). Fgf proteins such as Fgf8, Fgf17, Fgf18 and Fgf15, from the anterior telencephalon, have been shown to function as anterior patterning molecules (43–46). Among these growth factors, the role of Fgf8 has been extensively studied and it has been shown that Shh signaling is required to maintain robust Fgf8 expression (47,48). We therefore asked whether *Fgf8* expression is altered in *ShhN/+* telencephalon. As expected, we observed an expansion of *Fgf8* expression domain in the anterior forebrain of *ShhN/+* mutants as early as E9.5 (Fig. 5A, A′). At E10.5, the *Fgf8* expression domain encompassed the entire anterior telencephalic midline tissue in *ShhN/+* and even extended into the anterior diencephalon (Fig. 5B, B′).

One critical function of Fgf8 in the anterior neural ridge is to restrict Bmp signaling expression to the dorsal midline (18). Bmp signaling, in turn, is thought to promote localized cell death and the differentiation of a dorsal midline derivative, the choroid plexus, from roof plate progenitors (11,13). Thus, defective Bmp signaling could explain some of the midline defects observed in *ShhN/+* telencephalon despite expansion of roof plate progenitors. To test this possibility, we compared *Bmp4* expression and Bmp signaling activity in early wild-type and *ShhN/+* telencephalon. *Bmp4* expression was monitored using a sensitive *lacZ* reporter driven by the endogenous *Bmp4* promoter (49). At E9.5, a stage at which there was no evident morphological dorsal midline defect in *ShhN/+* (Fig. 1E, E′, F, F′), a reduction in *Bmp4*-expressing domain was already apparent in the dorsal telencephalic midline (arrowhead in Fig. 5C, C′). This reduction of *Bmp4* expression appeared to correlate with the lack of cell death at this stage (Fig. 1F′). By E10.5, the *Bmp4* reduction was more pronounced and extended to the rostral diencephalon (Fig. 5D, D′). Similarly, *in situ* analysis of *Bmp4* transcript also showed barely detectable level in the dorsal–medial telencephalon of *ShhN/+* mutants, in contrast to its robust expression in wild-type (Fig. 5E, E′). Concomitantly, the expression of *Msx1*, which correlates with sites of elevated Bmp signaling (5,11), was also significantly reduced in *ShhN/+* mutants (Fig. 5F, F′). Since it has been shown that nuclear accumulation of phosphorylated forms of Smad1, 5, 8 proteins (pSmads) is an indication of active Bmp signaling (50), we also determined pSmads expression by immunostaining. At E10.5, we observed significant accumulation of nuclear pSmads in the neuroepithelium of wild-type hippocampal primordium (white arrows in Fig. 5G) in contrast to its low level in the roof plate region. However, we did not detect high level of pSmads in *ShhN/+* dorsal telencephalic neuroepithelium, suggesting a severe loss of Bmp signaling. Notably, *ShhN/+* dorsal telencephalic mesenchymal cells also showed significantly reduced pSmads staining (Fig. 5G, G′, data not shown). Taken
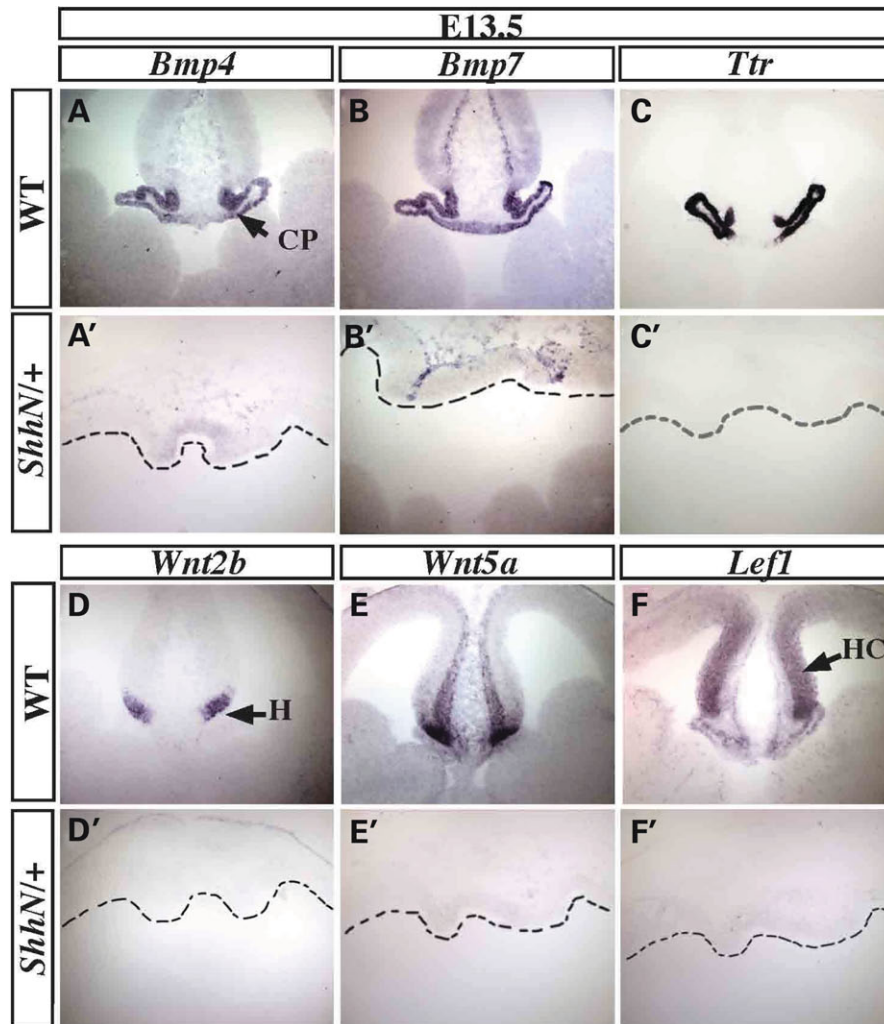
Figure 3. Loss of telencephalic choroid plexus, cortical hem and hippocampus in *ShhN/+* (**A**–**C**). Strong expressions of *Bmp4*, *Bmp7* and *Ttr* are detected in wild-type choroid plexus at E13.5 (**A′**–**C′**) Faint or no *Bmp4*, *Bmp7* and *Ttr* transcript signals are detected in *ShhN/+* dorsal midline; (**D**, **D′**, **E**, **E′**) Strong expressions of *Wnt2b* and *Wnt5a*, which demarcate Wnt-rich cortical hem, are significantly reduced in *ShhN/+*. (**F**, **F′**) A hippocampal precursor marker *Lef1* is similarly reduced in *ShhN/+*. The absence of *in situ* hybridization signals is not due to mRNA degradation in *ShhN/+* sections as their expressions are clearly present in other areas in the same section (e.g. strong *Bmp4* expression were present in the *ShhN/+* palatal epithelium, data not shown).

together, these findings indicate that deficient Bmp signaling at the dorsal midline likely accounts for the reduced cell death and defective choroid plexus formation in *ShhN/+* telencephalon.

The cortical hem, a developmentally transient structure positioned ventral to the hippocampus and dorsal to the telencephalic choroid plexus, is a source of multiple Wnt proteins that have also been implicated in dorsal midline development (15,39). Expanding the *Fgf8* expression domain by *in utero* electroporation suppressed the expression of *Wnts* (*Wnt2b*, *Wnt3a*, *Wnt5a*) in the cortical hem and led to a hypoplastic hippocampus. Thus, constraining the *Fgf8* expression boundary is vital for the maintenance of hem Wnt signaling and hippocampus development (14). Therefore, we asked whether expanded *Fgf8* expression and loss of high level Bmp signaling would impair Wnt signaling in *ShhN/+* dorsal telencephalon. *In situ* hybridization analyses showed that, while *Wnt2b*, *Wnt3a*, *Wnt5a* delineated the

Wnt-rich hem of wild-type dorsal midline at E10.5 and E11.5, their expressions were markedly diminished in *ShhN/+* mutants (Fig. 5H, H′, J, J′, K, K′). Notably, comparable expression of *Wnt7a* that is normally expressed at the lateral and dorsal cortex (39), but not the cortical hem, was observed in wild-type and *ShhN/+* (data not shown), indicating a specific loss of *Wnt* genes in the dorsal midline region. The severe loss of Wnt signaling activity in *ShhN/+* dorsal telencephalon was confirmed using TOPGAL reporter mice, which express β-galactosidase under the control of multimerized LEF/TCF consensus binding sites (Fig. 5I, I′, L, L′). The absence of apparent Wnt signaling activity may account for the severely defective hippocampal development in *ShhN/+* mutants.

Taken together, we conclude that ectopic ShhN signaling in the dorsal telencephalic region specifically impaired Bmp and Wnt signaling from dorsal patterning centers, likely via upregulation of *Fgf8* expression.
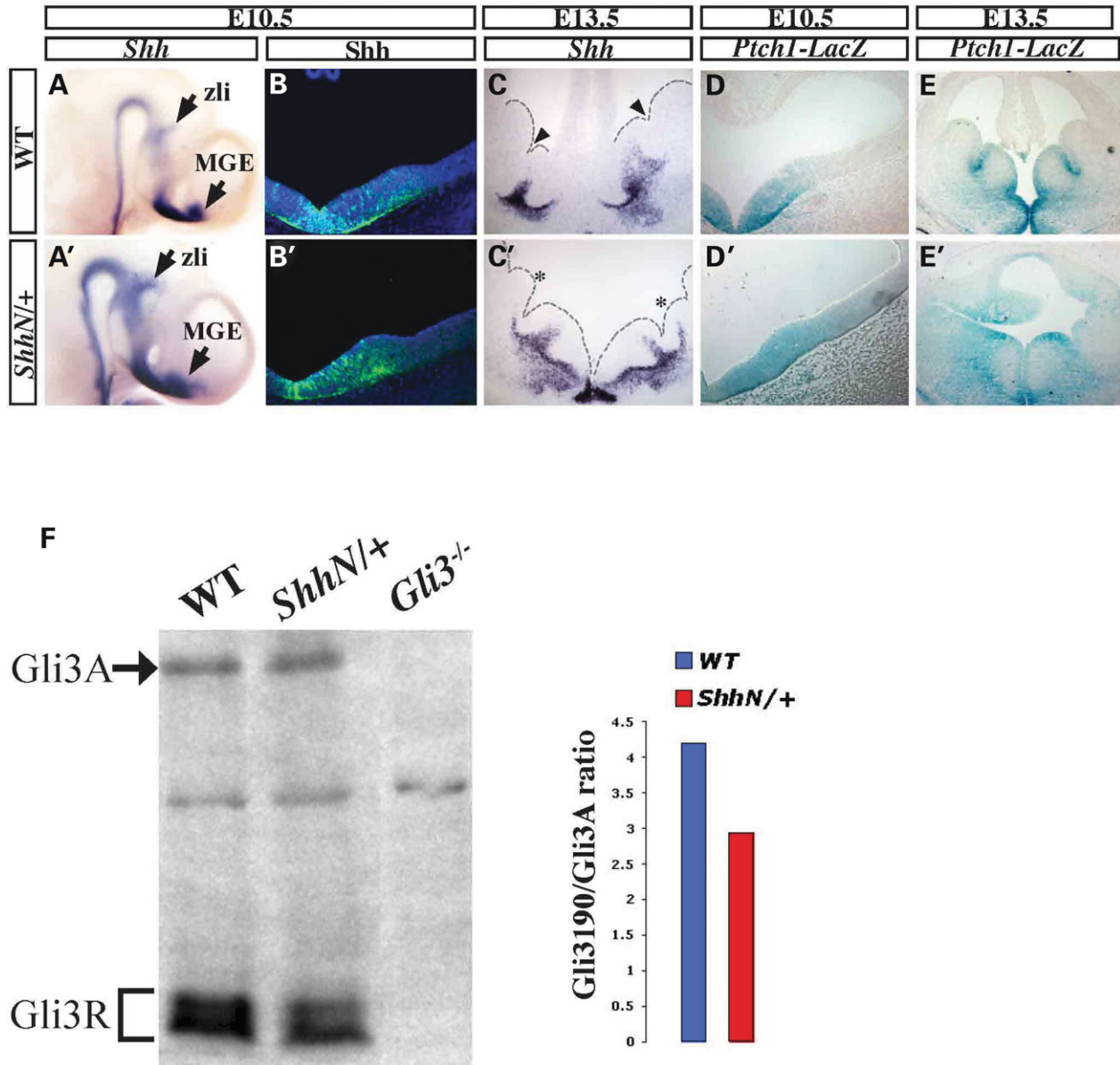
Figure 4. Widespread activation of Shh signaling in *ShhN*/+ telencephalon (**A**, **A'**, **B**, **B'**, **C**, **C'**) *Shh* transcript and Shh protein expression in wild-type (A–C) and *ShhN*/+ (A'–C'). Whole-mount *in situ* staining of Shh reveals a generally similar pattern between wild-type and *ShhN*/+; however, a modest expansion of *Shh* expression in MGE and zona limitans intrathalamica is observed in *ShhN*/+ when compared with wild-type (arrows in A and A'). Consistently, *Shh*-expressing domain extends into the ventral portion of the second ventral eminence in *ShhN*/+ (C'), while *Shh* transcript signal is confined within the MGE domain in wild-type (C). (B and B') Shh protein signal is detected mainly within the MGE region in both wild-type and *ShhN*/+. At E10.5, Shh signaling activity, as evidenced by *Ptch1-LacZ* expression, is confined within the MGE region in wild-type (**D**), but is extended in *ShhN*/+ (**D'**). At E13.5, *Ptch1-LacZ* expression is strongly expressed in the MGE and only weakly in the LGE (**E**), but in *ShhN*/+, the weak LGE expression extends to the entire cortical region including dorsal midline (**E'**). (**F**) Immunoblotting of whole brain protein extracts from E13.5 wild-type and *ShhN*/+ followed by incubation with Gli3-specific antibody recognizing Gli3 full-length (Gli3190) and repressor forms (Gli3R); *Gli3⁻/⁻* brain extract is used as negative control. Histogram shows relative Gli3R/Gli3190 ratio.

ShhN/+ mice display a spectrum of phenotypic features mimicking the human HPE

Next, we characterized the *ShhN*/+ forebrain and craniofacial defects at perinatal stages. Surprisingly, *ShhN*/+ mice showed relatively normal external craniofacial morphological defects, although a bulging cranium, which is generally associated with hydrocephalus (51), was clearly evident in more than

10 embryos examined (Fig. 6A, A'). Gross analysis of brains indicated an enlarged forebrain (and midbrain) and lack of olfactory bulbs in mutants (Fig. 6B, B'). H&E staining of coronal sections revealed that the enlarged ventral eminences in *ShhN*/+ were well separated (Fig. 6C, C'), whereas the dorsal midline of *ShhN*/+ telencephalon was severely hypoplastic and lacked conjunction of corpus callosum and septum that normally separated anterior cerebral hemispheres
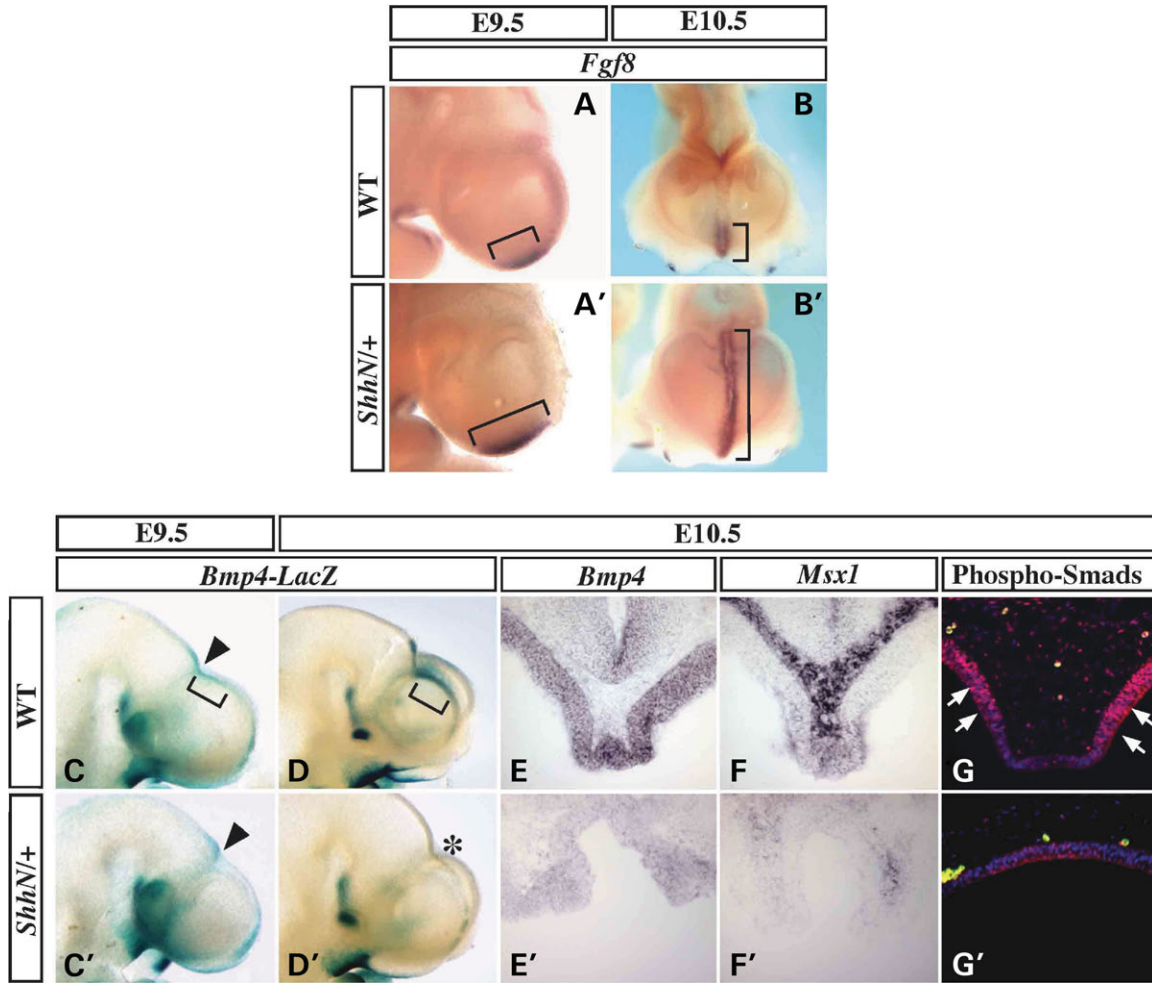
Figure 5. Upregulation of *Fgf8* in rostral midline accompanies loss of Bmp and Wnt signaling from dorsal organizing centers in *ShhN/+* telencephalon (**A**, **A′**, **B**, **B′**). Expansion of *Fgf8* expression. *Fgf8* expression is normally confined to the ventral anterior telencephalic midline at E9.5 (A) and E10.5 (B). However, in *ShhN/+*, *Fgf8* expression expands gradually to the entire dorsal–ventral axis of the anterior telencephalic midline (A′, B′). (**C**, **C′**, **D**, **D′**, **E**, **E′**, **F**, **F′**, **G**, **G′**) Loss of high-level Bmp4 expression and Bmp signaling in *ShhN/+* telencephalic dorsal midline. *Bmp4-LacZ* expression is detected in rostral diencephalons, but largely absent in the *ShhN/+* telencephalic dorsal midline at E9.5 (C′), while its expression is prominent in wild-type dorsal telencephalon (bracket in C) Arrowheads in (C) and (C′) indicate telencephalic–diencephalic boundary. *Bmp4-LacZ* expression is essentially abolished in *ShhN/+* dorsal midline and rostral diencephalic region at E10.5 (D, D′). *In situ* staining of *Bmp4* also reveals drastically reduced expression in *ShhN/+* (E′), in contrast to its robust expression in dorsal midline neuroepithelium of wild-type (E). Similar downregulation of *Msx1* is also observed (compare F and F′). Accordingly, nuclear accumulation of phosphorylated forms of Smad1, 5, 8 is largely abolished in *ShhN/+* dorsal neuroepithelium and adjacent mesenchymal cells (G, G′). (**H**, **H′**, **I**, **I′**, **J**, **J′**, **K**, **K′**, **L**, **L′**) Loss of multiple Wnt ligand expressions and canonical Wnt signaling in *ShhN/+* dorsal telencephalons. Dorsal midline tissue-specific expressions of Wnt ligands, including *Wnt2b*, *Wnt3a* and *Wnt5a*, are largely absent in *ShhN/+* (H, H′, J, J′, K, K′). As a result, canonical Wnt signaling, revealed by β-galactosidase activity in TOPGAL reporter mice (I, L), is largely abolished except in the small region of the posterior telencephalon (I′, L′). Dashed lines in (K) and (K′) indicate sectioning planes shown in (L) and (L′), respectively.

(Fig. 6C, C′). Dorsal interhemispheric cyst-like structure was occasionally observed in *ShhN/+* telencephalon (arrow in Fig. 6C′). In addition, the dorsal telencephalon of *ShhN/+* mutants lacked middle anterior commissure and characteristic choroid plexuses and hippocampal structures seen in wild-types (Fig. 6E, E′). Nevertheless, a small region of simplified epithelium with *Ttr* expression in the dorsal midline of the anterior forebrain in the newborn mutant was observed (Fig. 6F, F′). Since *Ttr* expression was absent in E13.5 *ShhN/+* mutants, this observation suggests either delayed/defective choroidal fate specification or a diencephalic origin of the choroid plexus. Regardless, the presence of low but persistent level of Bmp signaling in the roof region

(shown as residual Bmp4 and Bmp7 expressions at E10.5 in Fig. 5E, E′ and at E13.5 in Fig. 3A, A′, B, B′) likely contributed to the reduced choroidal fate in the mutant. Similarly, the development of the hippocampus was also significantly compromised. The expression of Prox1 marks the characteristic V-shape dentate gyrus of the hippocampus; we observed few and scattered Prox1+ cells at the distal cortical neuroepithelium in *ShhN/+* (Fig. 6G, G′), consistent with significantly reduced *Lef1* expression in the hippocampal precursors (Fig. 3F′).

In contrast to a monoventricle in the anterior telencephalon, the ventricles in the posterior telencephalon are clearly separated by an enlarged thalamus (Fig. 6D, D′). The identity of the
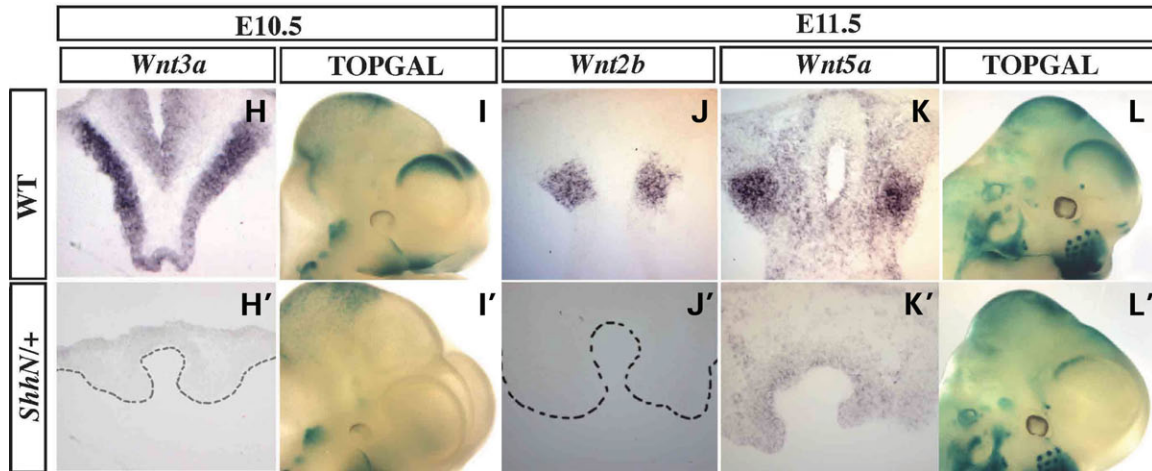
Figure 5. Continued.

thalamus was confirmed with Prox1 staining which is also expressed in the ventral–lateral thalamic region (Supplementary Material, Fig. S2). Although external craniofacial morphology appeared relatively unaffected, *ShhN*/+ mutants developed CLP. The palatal shelves failed to fuse in *ShhN*/+ at E15.5 (Fig. 6H, H′), leading to a cleft secondary palate in newborn pups (Fig. 6I, I′, J, J′). Strikingly, some of the phenotypic features including partial separation of the forebrain ventricles, hydrocephalus and CLP are similar to those found in a human patient with milder HPE carrying a truncation mutation (CAG → TAG, Q209X) in one *SHH* allele that was predicted to produce SHHN protein due to failure to catalyze cholesterol transfer; the other *SHH* allele was normal, thus indicating that the genotype of this patient is *SHHN*/+ (52).

DISCUSSION

HPE is the most common developmental anomaly of the human forebrain (21). Considerable amount of effort has been exerted to understand the pathogenesis of HPE, and several animal models that are generally associated with loss of Shh signaling have been established, showing severely disrupted ventral forebrain as a phenotypic hallmark. Our finding that *ShhN*/+ mice exhibit many aspects of forebrain defects observed in a human patient with a milder form of HPE with a similar genotype, implicates a novel mechanism by which ectopic Shh signaling impairs dorsal forebrain development, resulting in non-cleavage of midline structures. In addition, our study may shed light on the molecular pathogenesis of MIH, a variant of HPE that preferentially shows disruption of telencephalic dorsal midline structures.

Ectopic Shh signaling impairs dorsal organizing center function

Early telencephalic regionalization is mediated by diffusible morphogenic ligands and graded transcription factor expressions (1–3). It has long been established that Shh signaling is essential for ventral telencephalic patterning (4).

Recent studies indicate that this requirement appears to be mediated through Fgf signaling, as deletion of Fgf8 or multiple Fgf receptors in the telencephalon leads to loss of ventral cell fates analogous to that of $Shh^{-/-}$ mutants (18,53). Thus, the expansion of *Fgf8* expression to the dorsal midline in *ShhN*/+ mutants is consistent with long-range activation of Shh signaling. Because Fgf signaling normally promotes cell survival by restricting *Bmp4* expression in the dorsal midline (11,54), the decrease in cell death in *ShhN*/+ is in agreement with significantly reduced Bmp signaling. In addition, impaired choroid plexus formation can also be attributed to defective Bmp signaling as Bmpr1a gain- and loss-of-function studies reveal that Bmpr1a is required for promoting choroidal fate by antagonizing cortical specification (13). The hippocampus is another midline-derived structure that is defective in *ShhN*/+ telencephalon. Studies of *Wnt3a* or *Lef1* mutants have demonstrated that high level of canonical Wnt signaling close to the hem is vital for normal hippocampus development (15,16,55). The ability of ectopic *Fgf8* to suppress *Wnt2b*, *Wnt3a* and *Wnt5a* expressions at the cortical hem (14) is also consistent with hippocampus hypoplasia observed in *ShhN*/+ telencephalon. While altered dorsal patterning centers in *ShhN*/+ can be logically connected to the expanded *Fgf8* expression via ectopic Shh signaling, considering the prominent role of Shh in promoting neuroepithelial cell proliferation (56,57), it remains possible that Shh signaling can also directly contribute to increase cell proliferation and reduced cell death observed at the dorsal midline, resulting in defective roof plate progenitor cell differentiation, and subsequently dampening roof signaling activities (Fig. 7).

ShhN/+ as a novel mouse model of human HPE

HPE is characterized by a spectrum of brain malformations in which the bilateral cerebral hemispheres fail to separate along the midline. One of the principle underlying mechanisms of HPE pathogenesis is the disruption of basal forebrain patterning associated with impaired Shh signaling during early embryogenesis (22). Indeed, molecular genetic analyses have
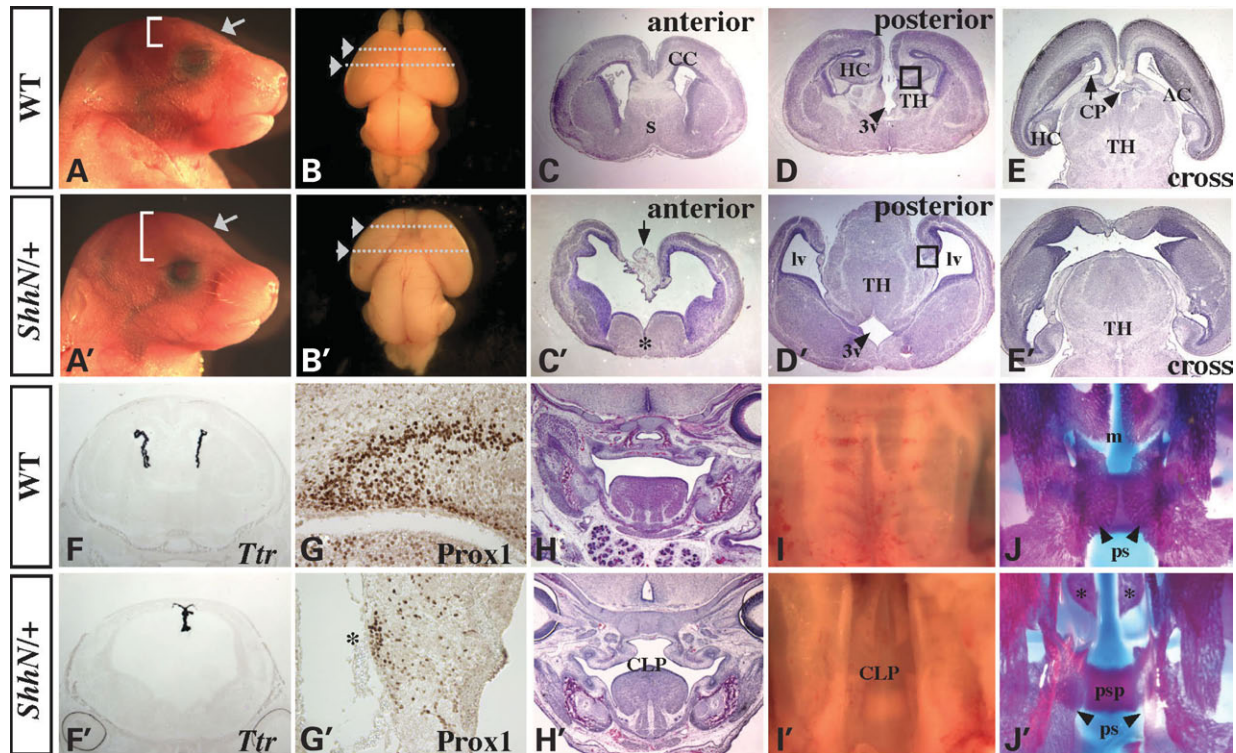
Figure 6. *ShhN*/+ mice mimic human HPE phenotypes. (**A**, **A′**) Wild-type and *ShhN*/+, both showing relatively normal external craniofacial morphologies except bulging forehead characteristic of hydrocephalus in mutant (white bracket in A′). (**B**, **B′**) Gross analysis of brains indicating lack of olfactory bulbs in mutant. (**C**, **C′**, **D**, **D′**) Coronal sections of wild-type and *ShhN*/+ telencephalons shown in (B) and (B′). In the rostral telencephalon, the corpus callosum (CC) and septum (s) that normally connect with each other to divide the telencephalic lobes into two lateral ventricles are either missing or defective in the mutant resulting in a single ventricle (compare C and C′). The mutant dorsal midline is severely hypoplastic with simplified epithelium and cyst-like structure (arrow). Note the presence of normally separated ventral eminences in *ShhN*/+. (C′). Caudally, *ShhN*/+ telencephalon lacks well-formed U-shaped hippocampus and the ventricles are separated by enlarged thalamus (D′). (**E**, **E′**) Brain cross-sections further show that the mutant lacks dorsal midline fissure, telencephalic choroid plexuses (CP) and anterior commissure (AC), while the separation of the thalamus (TH) is not affected. The simplified epithelium at the dorsal midline in *ShhN*/+ exhibits *Ttr* expression (**F′**), similar to the normal telencephalic choroid plexus in wild-type (**F**). (**G**) and (**G′**) were zoomed-in view of boxed-area shown in (D) and (D′). While Prox1 cells mark the characteristic V-shape dentate gyrus of the wild-type hippocampus (G), few and scattered Prox1 cells are found at the most distal *ShhN*/+ cortical neuroepithelium (G′) (**H**, **H′**, **I**, **I′**, **J**, **J′**) *ShhN*/+ mutants exhibit cleft secondary palate (CLP). E15.5 coronal section through the palatal region shows failure of palatal fusion in *ShhN*/+ (compare H to H′). A direct view of the secondary palate region with mandible removed shows cleft palate in *ShhN*/+ (compare I to I′). Skeletal staining further shows the presence of widely separated palatal shelves (J′), allowing direct view of the presphenoid bone (psp) underneath the otherwise fused palatine shelves. Note that the maxillary shelves are not fully mineralized in the mutant (asterisks) (J).

identified numerous SHH mutations in HPE patients, including a Q209X truncation mutation in one *SHH* allele that is predicted to produce SHHN protein (52). The Q209X patient was previously diagnosed with semi-lobar HPE, a milder form of HPE in which the brain is divided with two distinct hemispheres only in the caudal but not rostral region of the telencephalon (19–21). This patient also exhibited hydrocephalus and CLP; all of these phenotypic features are reproduced in the *ShhN*/+ mutant embryos. However, unlike 'classical' HPE, Shh signaling is ectopically activated and the basal forebrain is well separated in *ShhN*/+ mutants. Molecular analysis further revealed that the lack of regional cerebral hemispheric separation in *ShhN*/+ mutants is largely attributed to the disruption of dorsal midline signaling center. In this context, it is also interesting to note that dorsal midline defects have been reported in some patients with semi-lobar HPE (58). These observations suggest a novel mechanism by which ectopic Shh signaling could be associated with milder HPE.

Recent brain images and genetic studies in human have implicated an association of impaired embryonic roof plate development with MIH, a peculiar subtype of HPE, displaying non-cleavage of the cerebral hemisphere in the posterior frontal and parietal region. Notably, *ShhN*/+ mutants share several features observed in MIH patients, including: (i) largely normal craniofacial structures; (ii) frequent agenesis of the dorsal corpus callosum while ventral forebrain nuclei are generally separated; (iii) midline third ventricle is separated by hypothalamus at the posterior frontal lobe; (iv) dysgenesis of dorsal midline-derived structures including absence or reduced choroid plexus and hypoplastic hippocampus (23,25,26). We are only beginning to understand the molecular pathogenesis of MIH. The mechanism underlying the failure of hemispheric bifurcation in MIH appears to be different from that of classical HPE (22,23). In MIH, the defective functions of genetic factors impair roof plate development, whereas in classical HPE the floor plate is mostly affected. To date, the only gene implicated in MIH pathogenesis has been linked to mutations in *ZIC2*, which encodes a zinc finger protein that is homologous to *Drosophila* odd-paired (27). Reduced *Zic2* expression in mice results in
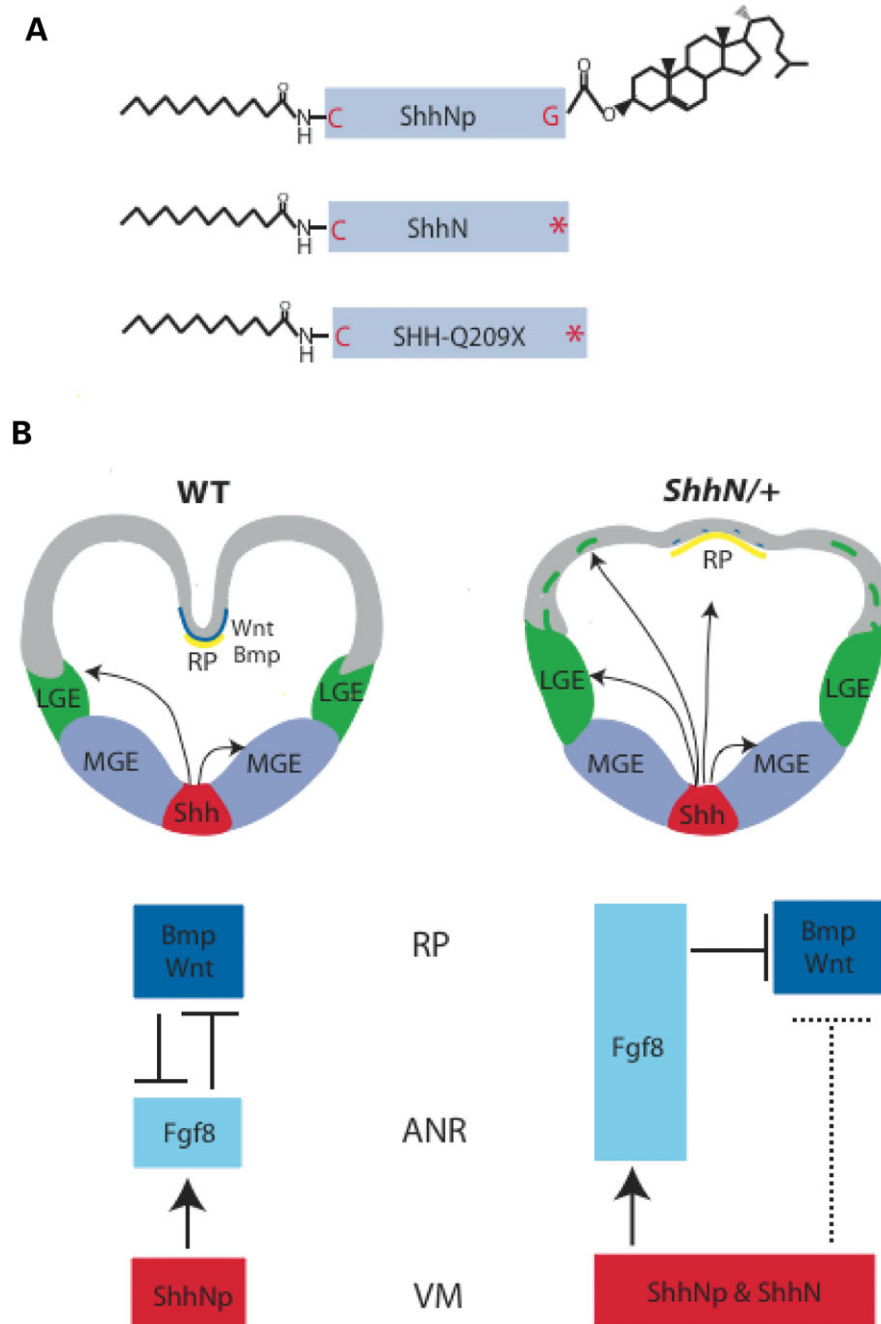
Figure 7. Proposed mechanism of dorsal midline dysgenesis and HPE mediated by ectopic Shh signaling. (**A**) Schematic of predicted protein products from mouse ShhN and human Q209X alleles. The mature Hh is synthesized as a precursor protein that undergoes a series of post-translational modifications, leading to covalent attachment of a cholesterol moiety at its carboxyl-terminus (Glycine 199) and palmitic acid at its N-terminal (72). In ShhN as well as SHH-Q209X, cholesterol modification does not occur due to deletion of the C-terminal processing domain of the precursor protein. (**B**) During normal development, Bmp and Wnt signals generated from the roof plate (RP) and its neighboring neuroepithelium are thought to pattern the dorsal midline structures such as choroid plexus, cortical hem and hippocampus (1). Shh secreted from the ventral telencephalic midline is required to maintain *Fgf8* expression in the anterio-ventral midline (anterior neural ridge, ANR). In turn Fgf8 restricts Bmp and Wnt signals to the dorsal midline (2). In *ShhN/+* mutants, widespread activation of Shh signaling activity leads to expansion of *Fgf8* expression to the dorsal midline, which in turn downregulates Bmp and Wnt signaling. In addition, long-range ShhN signaling may also directly promote cell proliferation and reduce cell death at the dorsal midline.

failure of roof plate invagination and fusion of cerebral hemispheres with relatively normal ganglionic eminence development (28). Indeed, it has been hypothesized that haplo-insufficiency in *ZIC2* underlies MIH in humans, and

the absence of craniofacial malformation, which is normally observed in mutants with loss of Shh signaling (23,27), argued that this anomaly may arise by an SHH-independent pathway. However, predominant ZIC2 mutations are

associated with classical HPE (27,59). The fact that *Zic2* ablation in mice does not faithfully reproduce MIH phenotypes (28), indicates that the molecular pathogenesis of MIH could be heterogeneous. Bmp and Wnt ligands derived from the roof region are thought to organize dorsal structures. Roof plate cell ablation leads to loss of dorsal midline-derived structures as well as associated Bmp signaling and thus, it has been proposed that *Bmp*s expressed in the roof plate are candidate genes for MIH (60). However, fate-mapping studies indicate that cells of the choroid plexus and Wnt-rich cortical hem are descendents of roof plate progenitors (12). Therefore, defective dorsal midline development could arise secondary to the depletion of roof plate cell population rather than a consequence of reduced Bmp signaling. Furthermore, studies of *Gdf7* (*Bmp12*) and telencephalon-specific conditional *Bmp4* and *Bmpr1a* mutants implicate a role of Bmp signaling primarily in choroid plexus specification and differentiation (12,13,61). Therefore, it remains an open question as to whether and how impaired Bmp signaling affects the intricate signaling network involved in dorsal telencephalic patterning that result in severe defects in multiple midline structures such as the choroid plexus, cortical hem and hippocampus observed in roof plate-depleted mutants. Our study demonstrates that reduced Bmp signaling coupled with impaired Wnt signaling appear to synergistically affect dorsal midline development. Thus, reduction in hem-enriched Wnt or its pathway activity should be considered as an integral part of MIH pathogenesis.

An intriguingly consistent phenotype of *ShhN/+* mice that parallels the phenotype observed in some human HPE patients, including MIH, is the CLP. Studies on *Fgf10*$^{-/-}$, *Fgfr2b*$^{-/-}$ and *Shh*$^{-/-}$ conditional mutant mice, all of which exhibit CLP, demonstrate that palatal epithelial *Shh* expression is a downstream target of *Fgf10* expressed in the palatal mesenchyme (62). Thus, loss of Shh signaling is generally associated with induction of CLP. However, *ShhN/+* mice exhibit Shh gain-of-function signaling in many developmental contexts such as in the telencephalon, spinal cord and limb bud (29) (this study and data not shown). Thus, the notion that Shh gain-of-function could also lead to CLP is particularly interesting. Recent investigation into *Insig1* and *Insig2* knockout mice also postulates that excess Shh signaling may cause CLP (63). Furthermore, hydrocephalus and CLP have been reported in several patients with a duplication of distal chromosome 7q, which contains the *SHH* gene locus, raising the possibility that overexpression of SHH may contribute to these craniofacial defects (64). Consistent with this notion, approximately 5% of Gorlin syndrome patients with PTCH1 mutations, in which Shh pathway activity is elevated, develop CLP (65). Further studies are required to determine the mechanism by which dysregulation of Shh signaling in *ShhN/+* leads to CLP formation. Similarly, how dysregulation of Shh signaling leads to absence of olfactory bulb in *ShhN/+* mutants remains to be determined. However, olfactory bulb aplasia has been observed in *Gli3* loss-of-function mutants (66–68), suggesting a causative link between loss of Gli3 repressor activity and failure of olfactory bulb development. Interestingly, olfactory bulb hypoplasia has also been reported in MIH patients (23).

MATERIALS AND METHODS

Animals

Generation of embryos expressing ShhN was carried out by mating *Shh*$^{\text{flox}/+}$ animals with *Sox2-Cre* deleter strain as previously described (29). *Sox2-Cre* (69), TOPGAL (70) and *Ptch1*^{lacZ} mice (40) were obtained from the Jackson Laboratory. *Bmp4*^{lacZ} mice were kindly provided by Brigid Hogan. The perinatal death of *Shh*$^{\text{flox}/\text{flox}}$, *ShhN/+* and *ShhN/−* mice precludes analysis of *ShhN/N* phenotype. Three to six embryos from wild-type and *ShhN/+* were used for each morphological/molecular analysis shown in each figure.

Immunohistochemistry and western analysis

All immunohistochemistry analyses were performed on tissue sections collected from OCT- or paraffin-embedded embryos as previously described (29). The primary antibodies were mouse anti-Pax6, (DSHB, 1:1), mouse anti-Nkx2.1, (Neomarkers, 1:100), mouse anti-Mash1 (gift of Jane Johnson, 1:100), goat anti-Shh (Santa Cruz Biotechnology, 1:1000), rabbit anti-phospho-Smad1/5/8 (gift of Tom Jessell and Ed Laufer, 1:1000), rabbit anti-Gsh2 (Kenneth Campbell, 1:1000), rabbit anti-Prox1 (Axxora, 1:500), mouse anti-Lhx1/5 (DSHB, 1:10). Since Lhx1 is not expressed in the telencephalon at early stages (71), the staining pattern shown in Figure 1 revealed Lhx5 expression pattern. For western analysis, protein lysate samples, 200 μg each, collected from E13.5 whole brains, were resolved on 6% SDS−polyacrylamide gels. Gli3−190 and Gli3R species were detected using a Gli3 N-terminal specific antibody as described (42).

Analysis of cell proliferation and apoptosis

BrdU (5-BromodeoxyUridine) *in vivo* labeling and TUNEL analysis were performed as previously described (71). For statistical analysis, three embryos from either wild-type or *ShhN/+* were used to perform BrdU and TUNEL analyses at each developmental stage. At least five stained sections were randomly selected and counted for each genotype to generate the proliferation and cell death indices shown in Figure 1. To assess differences among groups, statistical analyses were performed using a one-way analysis of variance (ANOVA) with Microsoft Excel (Microsoft Corporation) and significance accepted at $P < 0.05$. Results are presented as mean $\pm$ SEM.

X-gal staining and transcript detection

X-gal staining for β-galactosidase was performed according to standard protocol. Whole-mount and section *in situ* hybridizations were performed as described (71). The following cDNAs were used as templates for synthesizing digoxygenin-labeled riboprobes: *Shh*, *Lhx5* (H. Westphal, NIH), *Bmp4* (S. Lee, Johns Hopkins), *Bmp7* (E. Robertson, University of Oxford), *Msx1* (R. Mason, University of North Carolina), *Wnt3a* (Image 426103), *Wnt5a* (A. McMahon, Harvard University), *Wnt2b* (L. Zakin, Pasteur Institute), *Lef1* (R. Grossehedl, University of California San Francisco), *Fgf8* (G. Martin, University of California San Francisco), *Foxg1* (E. Lai, Cornell University), *Emx2* (A. Simeone,

European School of Molecular Medicine), Ttr (EST#1078224, ATCC).

Skeletal preparation

Cartilage and bones were stained with Alcian blue and Alizarin red as described (29).

SUPPLEMENTARY MATERIAL

Supplementary Material is available at HMG Online.

ACKNOWLEDGEMENTS

REFERENCES

1. Grove, E.A. and Fukuchi-Shimogori, T. (2003) Generating the cerebral cortical area map. *Annu. Rev. Neurosci.*, **26**, 355–380.
2. Sur, M. and Rubenstein, J.L. (2005) Patterning and plasticity of the cerebral cortex. *Science*, **310**, 805–810.
3. Campbell, K. (2003) Dorsal-ventral patterning in the mammalian telencephalon. *Curr. Opin. Neurobiol.*, **13**, 50–56.
4. Chiang, C., Litingtung, Y., Lee, E., Young, K.E., Corden, J.L., Westphal, H. and Beachy, P.A. (1996) Cyclopia and defective axial patterning in mice lacking Sonic hedgehog gene function. *Nature*, **383**, 407–413.
5. Shimamura, K. and Rubenstein, J.L. (1997) Inductive interactions direct early regionalization of the mouse forebrain. *Development*, **124**, 2709–2718.
6. Rallu, M., Machold, R., Gaiano, N., Corbin, J.G., McMahon, A.P. and Fishell, G. (2002) Dorsoventral patterning is established in the telencephalon of mutants lacking both Gli3 and Hedgehog signaling. *Development*, **129**, 4963–4974.
7. Gaiano, N., Kohtz, J.D., Turnbull, D.H. and Fishell, G. (1999) A method for rapid gain-of-function studies in the mouse embryonic nervous system. *Nat. Neurosci.*, **2**, 812–819.
8. Kohtz, J.D., Lee, H.Y., Gaiano, N., Segal, J., Ng, E., Larson, T., Baker, D.P., Garber, E.A., Williams, K.P. and Fishell, G. (2001) N-terminal fatty-acylation of sonic hedgehog enhances the induction of rodent ventral forebrain neurons. *Development*, **128**, 2351–2363.
9. Monuki, E.S. and Walsh, C.A. (2001) Mechanisms of cerebral cortical patterning in mice and humans. *Nat. Neurosci.*, **4** (suppl.), 1199–1206.
10. Lee, K.J. and Jessell, T.M. (1999) The specification of dorsal cell fates in the vertebrate central nervous system. *Annu. Rev. Neurosci.*, **22**, 261–294.
11. Furuta, Y., Piston, D.W. and Hogan, B.L. (1997) Bone morphogenetic proteins (BMPs) as regulators of dorsal forebrain development. *Development*, **124**, 2203–2212.
12. Currle, D.S., Cheng, X., Hsu, C.M. and Monuki, E.S. (2005) Direct and indirect roles of CNS dorsal midline cells in choroid plexus epithelia formation. *Development*, **132**, 3549–3559.
13. Hebert, J.M., Mishina, Y. and McConnell, S.K. (2002) BMP signaling is required locally to pattern the dorsal telencephalic midline. *Neuron*, **35**, 1029–1041.
14. Shimogori, T., Banuchi, V., Ng, H.Y., Strauss, J.B. and Grove, E.A. (2004) Embryonic signaling centers expressing BMP, WNT and FGF proteins interact to pattern the cerebral cortex. *Development*, **131**, 5639–5647.
15. Lee, S.M., Tole, S., Grove, E. and McMahon, A.P. (2000) A local Wnt-3a signal is required for development of the mammalian hippocampus. *Development*, **127**, 457–467.
16. Galceran, J., Miyashita-Lin, E.M., Devaney, E., Rubenstein, J.L. and Grosschedl, R. (2000) Hippocampus development and generation of dentate gyrus granule cells is regulated by LEF1. *Development*, **127**, 469–482.
17. Backman, M., Machon, O., Mygland, L., van den Bout, C.J., Zhong, W., Taketo, M.M. and Krauss, S. (2005) Effects of canonical Wnt signaling on dorso-ventral specification of the mouse telencephalon. *Dev. Biol.*, **279**, 155–168.
18. Storm, E.E., Garel, S., Borello, U., Hebert, J.M., Martinez, S., McConnell, S.K., Martin, G.R. and Rubenstein, J.L. (2006) Dose-dependent functions of Fgf8 in regulating telencephalic patterning centers. *Development*, **133**, 1831–1844.
19. Hayhurst, M. and McConnell, S.K. (2003) Mouse models of holoprosencephaly. *Curr. Opin. Neurol.*, **16**, 135–141.
20. Kinsman, S.L., Plawner, L.L. and Hahn, J.S. (2000) Holoprosencephaly: recent advances and new insights. *Curr. Opin. Neurol.*, **13**, 127–132.
21. Cohen, M.M., Jr. (2006) Holoprosencephaly: clinical, anatomic, and molecular dimensions. *Birth Defects Res. A Clin. Mol. Teratol.*, **76**, 658–673.
22. Muenke, M. and Beachy, P.A. (2000) Genetics of ventral forebrain development and holoprosencephaly. *Curr. Opin. Genet. Dev.*, **10**, 262–269.
23. Simon, E.M., Hevner, R.F., Pinter, J.D., Clegg, N.J., Delgado, M., Kinsman, S.L., Hahn, J.S. and Barkovich, A.J. (2002) The middle interhemispheric variant of holoprosencephaly. *Am. J. Neuroradiol.*, **23**, 151–156.
24. Barkovich, A.J. and Quint, D.J. (1993) Middle interhemispheric fusion: an unusual variant of holoprosencephaly. *Am. J. Neuroradiol.*, **14**, 431–440.
25. Lewis, A.J., Simon, E.M., Barkovich, A.J., Clegg, N.J., Delgado, M.R., Levey, E. and Hahn, J.S. (2002) Middle interhemispheric variant of holoprosencephaly: a distinct cliniconeuroradiologic subtype. *Neurology*, **59**, 1860–1865.
26. Pulitzer, S.B., Simon, E.M., Crombleholme, T.M. and Golden, J.A. (2004) Prenatal MR findings of the middle interhemispheric variant of holoprosencephaly. *Am. J. Neuroradiol.*, **25**, 1034–1036.
27. Brown, L.Y., Odent, S., David, V., Blayau, M., Dubourg, C., Apacik, C., Delgado, M.A., Hall, B.D., Reynolds, J.F., Sommer, A. *et al.* (2001) Holoprosencephaly due to mutations in ZIC2: alanine tract expansion mutations may be caused by parental somatic recombination. *Hum. Mol. Genet.*, **10**, 791–796.
28. Nagai, T., Aruga, J., Minowa, O., Sugimoto, T., Ohno, Y., Noda, T. and Mikoshiba, K. (2000) Zic2 regulates the kinetics of neurulation. *Proc. Natl Acad. Sci. USA*, **97**, 1618–1623.
29. Li, Y., Zhang, H., Litingtung, Y. and Chiang, C. (2006) Cholesterol modification restricts the spread of Shh gradient in the limb bud. *Proc. Natl Acad. Sci. USA*, **103**, 6548–6553.
30. Zhao, Y., Sheng, H.Z., Amini, R., Grinberg, A., Lee, E., Huang, S., Taira, M. and Westphal, H. (1999) Control of hippocampal morphogenesis and neuronal differentiation by the LIM homeobox gene *Lhx5*. *Science*, **284**, 1155–1158.
31. Shinozaki, K., Yoshida, M., Nakamura, M., Aizawa, S. and Suda, Y. (2004) Emx1 and Emx2 cooperate in initial phase of archipallium development. *Mech. Dev.*, **121**, 475–489.
32. Ericson, J., Rashbass, P., Schedl, A., Brenner-Morton, S., Kawakami, A., van Heyningen, V., Jessell, T.M. and Briscoe, J. (1997) Pax6 controls progenitor cell identity and neuronal fate in response to graded Shh signaling. *Cell*, **90**, 169–180.
33. Lo, L.C., Johnson, J.E., Wuenschell, C.W., Saito, T. and Anderson, D.J. (1991) Mammalian achaete-scute homolog 1 is transiently expressed by spatially restricted subsets of early neuroepithelial and neural crest cells. *Genes. Dev.*, **5**, 1524–1537.
34. Casarosa, S., Fode, C. and Guillemot, F. (1999) Mash1 regulates neurogenesis in the ventral telencephalon. *Development*, **126**, 525–534.
35. Horton, S., Meredith, A., Richardson, J.A. and Johnson, J.E. (1999) Correct coordination of neuronal differentiation events in ventral forebrain requires the bHLH factor MASH1. *Mol. Cell. Neurosci.*, **14**, 355–369.
36. Kohtz, J.D., Baker, D.P., Corte, G. and Fishell, G. (1998) Regionalization within the mammalian telencephalon is mediated by changes in responsiveness to Sonic Hedgehog. *Development*, **125**, 5079–5089.
37. Corbin, J.G., Gaiano, N., Machold, R.P., Langston, A. and Fishell, G. (2000) The Gsh2 homeodomain gene controls multiple aspects of telencephalic development. *Development*, **127**, 5007–5020.

38. Yun, K., Potter, S. and Rubenstein, J.L. (2001) Gsh2 and Pax6 play complementary roles in dorsoventral patterning of the mammalian telencephalon. *Development*, **128**, 193–205.

39. Grove, E.A., Tole, S., Limon, J., Yip, L. and Ragsdale, C.W. (1998) The hem of the embryonic cerebral cortex is defined by the expression of multiple Wnt genes and is compromised in Gli3-deficient mice. *Development*, **125**, 2315–2325.

40. Goodrich, L.V., Milenkovic, L., Higgins, K.M. and Scott, M.P. (1997) Altered neural cell fates and medulloblastoma in mouse patched mutants. *Science*, **277**, 1109–1113.

41. Wang, B., Fallon, J.F. and Beachy, P.A. (2000) Hedgehog-regulated processing of Gli3 produces an anterior/posterior repressor gradient in the developing vertebrate limb. *Cell*, **100**, 423–434.

42. Litingtung, Y., Dahn, R.D., Li, Y., Fallon, J.F. and Chiang, C. (2002) Shh and Gli3 are dispensable for limb skeleton formation but regulate digit number and identity. *Nature*, **418**, 979–983.

43. Maruoka, Y., Ohbayashi, N., Hoshikawa, M., Itoh, N., Hogan, B.L. and Furuta, Y. (1998) Comparison of the expression of three highly related genes, Fgf8, Fgf17 and Fgf18, in the mouse embryo. *Mech. Dev.*, **74**, 175–177.

44. Gimeno, L., Brulet, P. and Martinez, S. (2003) Study of Fgf15 gene expression in developing mouse brain. *Gene Exp. Patterns*, **3**, 473–481.

45. Bachler, M. and Neubuser, A. (2001) Expression of members of the Fgf family and their receptors during midfacial development. *Mech. Dev.*, **100**, 313–316.

46. Crossley, P.H., Martinez, S., Ohkubo, Y. and Rubenstein, J.L. (2001) Coordinate expression of Fgf8, Otx2, Bmp4, and Shh in the rostral prosencephalon during development of the telencephalic and optic vesicles. *Neuroscience*, **108**, 183–206.

47. Ohkubo, Y., Chiang, C. and Rubenstein, J.L. (2002) Coordinate regulation and synergistic actions of BMP4, SHH and FGF8 in the rostral prosencephalon regulate morphogenesis of the telencephalic and optic vesicles. *Neuroscience*, **111**, 1–17.

48. Aoto, K., Nishimura, T., Eto, K. and Motoyama, J. (2002) Mouse GLI3 regulates Fgf8 expression and apoptosis in the developing neural tube, face, and limb bud. *Dev. Biol.*, **251**, 320–332.

49. Weaver, M., Dunn, N.R. and Hogan, B.L. (2000) Bmp4 and Fgf10 play opposing roles during lung bud morphogenesis. *Development*, **127**, 2695–2704.

50. Feng, X.H. and Derynck, R. (2005) Specificity and versatility in tgf-beta signaling through Smads. *Annu. Rev. Cell. Dev. Biol.*, **21**, 659–693.

51. Banizs, B., Pike, M.M., Millican, C.L., Ferguson, W.B., Komlosi, P., Sheetz, J., Bell, P.D., Schwiebert, E.M. and Yoder, B.K. (2005) Dysfunctional cilia lead to altered ependyma and choroid plexus function, and result in the formation of hydrocephalus. *Development*, **132**, 5329–5339.

52. Nanni, L., Ming, J.E., Bocian, M., Steinhaus, K., Bianchi, D.W., Die-Smulders, C., Giannotti, A., Imaizumi, K., Jones, K.L., Campo, M.D. *et al.* (1999) The mutational spectrum of the sonic hedgehog gene in holoprosencephaly: SHH mutations cause a significant proportion of autosomal dominant holoprosencephaly. *Hum. Mol. Genet.*, **8**, 2479–2488.

53. Gutin, G., Fernandes, M., Palazzolo, L., Paek, H., Yu, K., Ornitz, D.M., McConnell, S.K. and Hebert, J.M. (2006) FGF signalling generates ventral telencephalic cells independently of SHH. *Development*, **133**, 2937–2946.

54. Storm, E.E., Rubenstein, J.L. and Martin, G.R. (2003) Dosage of Fgf8 determines whether cell survival is positively or negatively regulated in the developing forebrain. *Proc. Natl Acad. Sci. USA*, **100**, 1757–1762.

55. Zhou, C.J., Zhao, C. and Pleasure, S.J. (2004) Wnt signaling mutants have decreased dentate granule cell production and radial glial scaffolding abnormalities. *J. Neurosci.*, **24**, 121–126.

56. Ho, K.S. and Scott, M.P. (2002) Sonic hedgehog in the nervous system: functions, modifications and mechanisms. *Curr. Opin. Neurobiol.*, **12**, 57–63.

57. Stecca, B. and Ruiz i Altaba, A. (2005) Brain as a paradigm of organ growth: hedgehog-Gli signaling in neural stem cells and brain tumors. *J. Neurobiol.*, **64**, 476–490.

58. Takahashi, T., Kinsman, S., Makris, N., Grant, E., Haselgrove, C., McInerney, S., Kennedy, D.N., Takahashi, T., Fredrickson, K., Mori, S. *et al.* (2003) Semilobar holoprosencephaly with midline 'seam': a topologic and morphogenetic model based upon MRI analysis. *Cereb. Cortex*, **13**, 1299–1312.

59. Brown, S.A., Warburton, D., Brown, L.Y., Yu, C.Y., Roeder, E.R., Stengel-Rutkowski, S., Hennekam, R.C. and Muenke, M. (1998) Holoprosencephaly due to mutations in ZIC2, a homologue of *Drosophila* odd-paired. *Nat. Genet.*, **20**, 180–183.

60. Cheng, X., Hsu, C.M., Currle, D.S., Hu, J.S., Barkovich, A.J. and Monuki, E.S. (2006) Central roles of the roof plate in telencephalic development and holoprosencephaly. *J. Neurosci.*, **26**, 7640–7649.

61. Hebert, J.M., Hayhurst, M., Marks, M.E., Kulessa, H., Hogan, B.L. and McConnell, S.K. (2003) BMP ligands act redundantly to pattern the dorsal telencephalic midline. *Genesis*, **35**, 214–219.

62. Rice, R., Spencer-Dene, B., Connor, E.C., Gritli-Linde, A., McMahon, A.P., Dickson, C., Thesleff, I. and Rice, D.P. (2004) Disruption of Fgf10/ Fgfr2b-coordinated epithelial-mesenchymal interactions causes cleft palate. *J. Clin. Invest.*, **113**, 1692–1700.

63. Engelking, L.J., Evers, B.M., Richardson, J.A., Goldstein, J.L., Brown, M.S. and Liang, G. (2006) Severe facial clefting in Insig-deficient mouse embryos caused by sterol accumulation and reversed by lovastatin. *J. Clin. Invest.*, **116**, 2356–2365.

64. Morava, E., Bartsch, O., Czako, M., Frensel, A., Kalscheuer, V., Karteszi, J. and Kosztolanyi, G. (2003) Small inherited terminal duplication of 7q with hydrocephalus, cleft palate, joint contractures, and severe hypotonia. *Clin. Dysmorphol.*, **12**, 123–127.

65. Evans, D.G., Ladusans, E.J., Rimmer, S., Burnell, L.D., Thakker, N. and Farndon, P.A. (1993) Complications of the naevoid basal cell carcinoma syndrome: results of a population based study. *J. Med. Genet.*, **30**, 460–464.

66. Franz, T. (1994) Extra-toes (Xt) homozygous mutant mice demonstrate a role for the Gli-3 gene in the development of the forebrain. *Acta Anat. (Basel)*, **150**, 38–44.

67. Tomioka, N., Osumi, N., Sato, Y., Inoue, T., Nakamura, S., Fujisawa, H. and Hirata, T. (2000) Neocortical origin and tangential migration of guidepost neurons in the lateral olfactory tract. *J. Neurosci.*, **20**, 5802–5812.

68. Naruse, I. and Keino, H. (1993) Induction of agenesis of the corpus callosum by the destruction of anlage of the olfactory bulb using fetal laser surgery *ex utero* in mice. *Brain Res. Dev. Brain Res.*, **71**, 69–74.

69. Hayashi, S., Lewis, P., Pevny, L. and McMahon, A.P. (2002) Efficient gene modulation in mouse epiblast using a *Sox2-Cre* transgenic mouse strain. *Mech. Dev.*, **119** (Suppl. 1), S97–S101.

70. DasGupta, R. and Fuchs, E. (1999) Multiple roles for activated LEF/TCF transcription complexes during hair follicle development and differentiation. *Development*, **126**, 4557–4568.

71. Li, Y., Zhang, H., Choi, S.C., Litingtung, Y. and Chiang, C. (2004) Sonic hedgehog signaling regulates Gli3 processing, mesenchymal proliferation, and differentiation during mouse lung organogenesis. *Dev. Biol.*, **270**, 214–231.

72. Mann, R.K. and Beachy, P.A. (2004) Novel lipid modifications of secreted protein signals. *Annu. Rev. Biochem.*, **73**, 891–923.